ASTRONOMY & ASTROPHYSICS
SUPPLEMENT SERIES

Astron. Astrophys. Suppl. Ser. **127,** 167-179 (1998)

V, I CCD photometry of metal-rich globular clusters: NGC 6528⋆

T. Richtler[1,2], E.K. Grebel[1,3], A. Subramaniam[2], and R. Sagar[2,4]

[1] Sternwarte der Universität Bonn, Auf dem Hügel 71, D-53121 Bonn, Germany
richtler@astro.uni-bonn.de
[2] Indian Institute of Astrophysics, 560034 Bangalore, India
purni@iiap.ernet.in, sagar@iiap.ernet.in
[3] Astronomisches Institut der Universität Würzburg, Am Hubland, D-97074 Würzburg, Germany
grebel@astro.uni-wuerzburg.de
[4] Uttar Pradesh State Observatory, Naini Tal, India

Received October 11, 1995; accepted April 29, 1997

Abstract. We present CCD photometry in V and I for the metal-rich globular cluster NGC 6528. A comparison with previous photometry reveals discrepancies of the order 0.1 to 0.2 mag in V, emphasizing the need for independent photometry. As found previously, the giant branch (or the asymptotic giant branch, which cannot be distinguished) of the cluster extends to $V - I = 7$. Population synthesis in $V-I$ must take these red stars into account in order to understand integrated red colours of bulge populations. Currently available theoretical isochrones do not reproduce the shape of the RGB/AGB. The derivation of reliable values for reddening, distance and metallicity of NGC 6528 is hampered by uncertainties in the extrapolation to high metallicity, which dominate the absolute error rather than the photometric uncertainty does. Together with other properties (old age derived from HST data, high radial velocity), this object is more likely a member of the bulge than of the disk population.[1]

Key words: Galaxy: globular clusters: general; individual: NGC 6528 — galaxy abundances — stars: late-type — HR diagram

1. Introduction

Most Galactic globular clusters are (even paradigmatic) representatives of the Galactic halo population. However, there is a sample of globular clusters, for which considerable uncertainty exists with respect to their role in evolution and structure of the Milky Way.

Clusters more metal-rich than −0.8 dex (on the scale of Zinn & West 1984) have been assigned to the "disk" population of globular clusters (Zinn 1985; Armandroff 1993). Other authors (Ortolani et al. 1992; Minniti 1995) in contrast see them as "bulge" clusters. Burkert & Smith (1997) even discuss substructure among this group. Apart from 47 Tuc and M 71, few spectroscopic abundance determinations based on individual stars have been carried out. François (1991) obtained [Fe/H] = −0.9 dex for one star in NGC 5927 and Barbuy et al. (1992) measured [Fe/H] = −0.2 dex for one star in NGC 6553. Fullton et al. (1995) investigated NGC 6352 and found it very similar to 47 Tuc. Many of these clusters are seen in projection onto the Galactic bulge, which means severe contamination by field stars. For these clusters, abundances are still mainly based on integrated colours if available at all. Additionally, the clusters are strongly reddened, which complicates the interpretation of both colour-magnitude diagrams (CMDs) and spectroscopy. Therefore, the metallicity scale of globular clusters in the metal-rich domain is not yet well established.

Richtler et al. (1994) investigated the clusters NGC 6496, NGC 6624, and NGC 6637 (M 69) and found them to be distinctly more metal-poor than what had been previously suggested. Also their minimal orbit inclinations do not indicate an association with the Galactic disk. More and better information about these difficult objects is clearly needed to understand their role within the Galactic globular cluster system.

NGC 6528 is particularly difficult to analyze. On the scale of Zinn & West (1984), it holds the record with a metallicity of +0.2 dex. An early photographic study

Send offprint requests to: T. Richtler, Bonn

⋆ Based on observations obtained at the European Southern Observatory, La Silla, Chile.

[1] Table 6 containing the photometry of individual stars is only available in electronic form via anonymous ftp 130.79.128.5 or http: //cdsweb.u-strasbg.fr/Abstract.html

from van den Bergh & Younger (1979) found the cluster to be quite metal-rich, but the usefulness of photographic data in such crowded fields is very limited. Armandroff & Zinn (1988) determined the metallicity of NGC 6528 to be −0.23 dex based on the infrared Ca triplet in integrated cluster spectra. Ortolani et al. (1992) (herafter OBB) give results for metallicity, reddening, and distance together with other basic cluster data.

The turn-off region is not clearly identifiable even in the CCD CMDs of OBB. Thus the question of whether NGC 6528 could be younger than the majority of galactic globular clusters, as has been suggested for disk globular clusters, remained unanswered. After the first version of our paper was submitted, Ortolani et al. (1995) published HST observations of NGC 6528, showing unambiguously the turn-off of the main sequence location. They also estimated the age placing NGC 6528 among the old globular clusters of the Galaxy. Also for NGC 6352, another "disk cluster", an old age has been found (Fullton et al. 1995).

Regarding the turn-off location, the HST data is clearly superior over ground based data. We thus dropped the discussion of the age completely. However, the metallicity could not be quantified in the HST study beyond the statement that it is a quite metal-rich cluster.

A remarkable feature pointed out in the study of OBB is the "curved giant branch", which OBB attribute to strong blanketing due to the high metallicity of that cluster. They even locate the red giant branch tip at a V-band brightness fainter than the horizontal branch. These peculiarities together with the fact that this cluster may be at the upper end of the metallicity scale of globular clusters makes an independent study worthwhile.

Table 1. Basic cluster data for NGC 6528

Parameter	value	reference
RA (2000)	$18^{\rm h}1^{\rm m}37\overset{\rm s}{.}2$	
Dec (2000)	$-30^\circ3'25''$	
$l_{\rm II}$	$1\overset{\circ}{.}14$	
$b_{\rm II}$	$-4\overset{\circ}{.}17$	
$E(B-V)$	0.55	Ortolani et al. (1992)
Distance [kpc]	7.5	Ortolani et al. (1992)
[Fe/H]	-0.23 ± 0.11	Armandroff & Zinn (1988)
$v_{\rm r}$	+189 km/s	Armandroff & Zinn (1988)

2. Observations and reductions

The data were obtained with the 2.2 m MPIA telescope at the European Southern Observatory (ESO) at La Silla, Chile. We carried out our observations during two nights, the 18th and 19th of July, 1993. We used the ESO Faint Object Spectrograph and Camera (EFOSCII) equipped with a 1 K Thomson CCD (ESO #19). The pixel scale of this CCD is $0\overset{''}{.}332$ resulting in a field of view of $5.7' \times 5.7'$. ESO filters 584 and 618 were used, which are Bessell V and Gunn i. Table 2 gives a log of the observations. Figure 1 shows the identification chart for the imaged cluster region. The seeing was slightly below $1''$ on the short exposure frames and about $1\overset{''}{.}1$ to $1\overset{''}{.}2$ arcsec in all of the 3 min exposures.

Table 2. Observing log for NGC 6528

Filter	exp.time	no. of frames	date
V	60 s	1	18 July 93
V	180 s	6	18 July 93
I	30 s	1	18 July 93
I	180 s	5	18 July 93
I	30 s	2	19 July 93
V	30 s	2	19 July 93
I	216 s	1	19 July 93
I	180 s	3	19 July 93
V	180 s	4	19 July 93

In addition, 16 stars from the list of Landolt (1992) selected by M. Bessell for telescopes with small fields of view were repeatedly observed. Although our filters differ from the filters used by Landolt, we could reproduce the Landolt system quite well, at least below the limits which are implied by the photometric quality. Although the observations in the first night were obtained in clear conditions, the photometric quality was not as good as in the second night. Therefore we relied on the second night alone for the photometric transformation.

Twilight flat fields were used for all flat fielding. All photometric reductions were done using the DAOPHOT II profile fitting software (Stetson 1992). Further processing and conversion of these raw instrumental magnitudes to the standard photometric system were performed using the procedure outlined by Stetson (1992).

In deriving the colour equation for the CCD system and evaluating the zero-points for the data frames, nightly values of atmospheric extinction were used, which were simultaneously calculated with colour equations and zero points and were found to agree well with the standard values for La Silla, pointing to the photometric quality of the run. The colour equations for the CCD system were determined by performing aperture photometry on the Landolt's standards, which cover a sufficiently wide range in colour. A linear regression yields the following colour equations:

$$\Delta V_{\rm CCD} = \Delta V - 0.067(V-I)$$

$$\Delta I_{\rm CCD} = \Delta I + 0.045(V-I)$$

where V and I are standard magnitudes taken from Landolt (1992) and $V_{\rm CCD}$ and $I_{\rm CCD}$ are CCD aperture

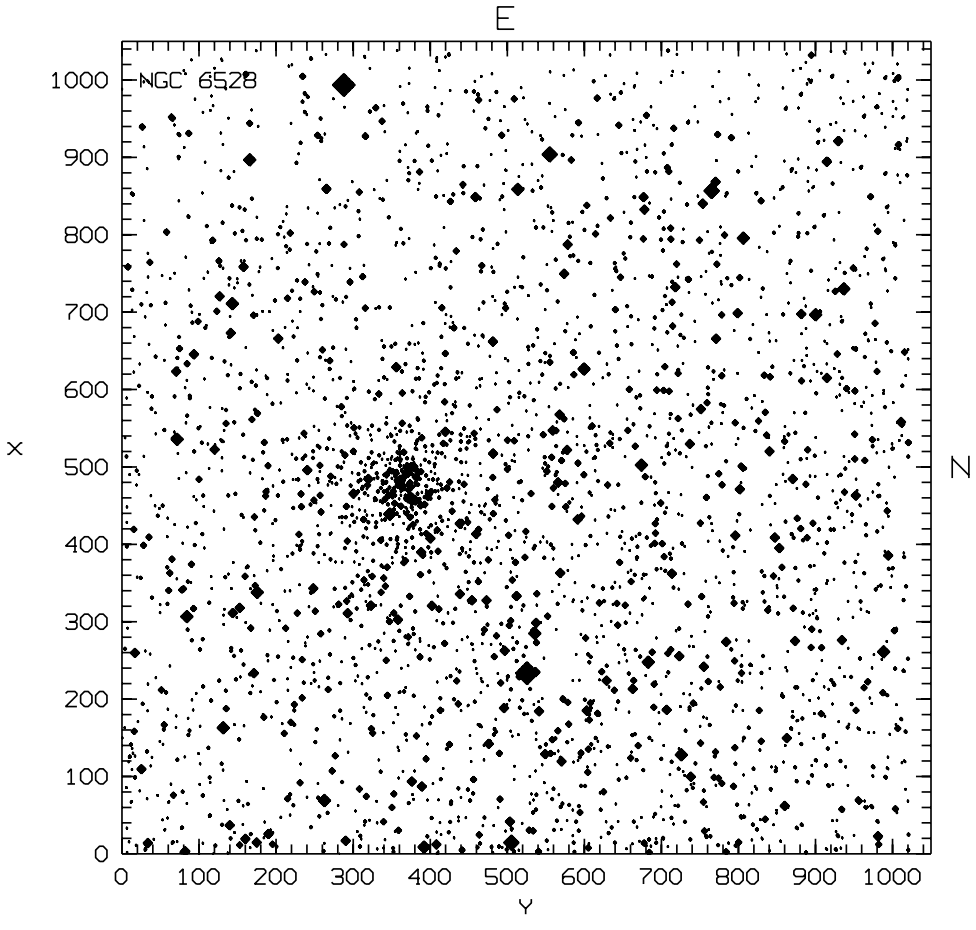

Fig. 1. A finding chart for our field centered on NGC 6528. Seven different symbol sizes are used to represent the magnitude range from $V = 13$ to 19 mag. North is up, west is right. Identification of stars is feasible via a short list of the brightest stars (Table 3). The field of view is $5.7' \times 5.7'$. Some stars have large errors due to crowding or location at the frame edge. We left them in to facilitate the identification

magnitudes. For establishing the local standards, we selected about 40 stars on the reference frame, which according to brightness and the absence of close neighbours could serve as "secondary standards" in the sense of Stetson's calibration procedures. All other stars were subtracted from the frame, thus alleviating the difficulties caused by the severe crowding of stars.

For determining the difference between aperture and PSF-magnitudes, aperture "curves-of-growth" were constructed using the DAOGROW programme (Stetson 1990). These differences and difference in exposure time and atmospheric extinction were used for determining the standard magnitudes of "local standards", i.e. selected stars on the frame, which are suitable for computing the difference between PSF- and aperture magnitudes. Using these local standards, the profile magnitudes were transformed to the standard system. The zeropoints are uncertain by ~ 0.03 mag in V and ~ 0.02 mag in I, which is the dispersion of the frame-to-frame scatter.

2.1. Comparison with previous measurements

We can compare our photometry with that of OBB because S. Ortolani kindly provided us with a computer-readable table of their photometric results. The transformation equations relating the OBB ($X_{\rm OBB}$, $Y_{\rm OBB}$) coordinate system top ours ($X_{\rm pres}$, $Y_{\rm pres}$) are:

$$X_{\rm OBB} = -153.406 + 0.716 X_{\rm pres} - 0.004 Y_{\rm pres}$$

$$Y_{\rm OBB} = -12.089 + 0.004 X_{\rm pres} + 0.716 Y_{\rm pres}.$$

There are 1343 stars in the OBB data whose positions coincide within 1 pixel with the stars measured by us. The differences between the data are given in Table 4. Except for a few outliers, which appear to be mostly those treated as single in our measurements and as blended doubles in theirs, the distribution of the photometric differences indicates a constant zero-point offset of about 0.14 mag for stars brighter than $V \sim 19$ mag, which becomes as large as 0.27 mag for stars with $V \sim 21$ mag. There seems to be good agreement between the two sets of data in $V - I$ for stars brighter than 18 mag.

Table 3. List of stars brighter than $V = 15.5$ for identification and comparison purposes. Given are the X, Y-coordinates (appearing in Fig. 1, V, $V-I$, and the respective photometric errors as given by DAOPHOT. Some stars have large photometric errors due to crowding or location at the frame edge

No.	X	Y	V	σV	$V-I$	$\sigma V-I$
1	+204.88	−21.57	15.458	+.071	1.024	+.075
2	+535.66	+71.56	14.022	+.018	+.660	+.019
3	+1.92	+81.05	15.183	+.061	+.177	+.163
4	+3.30	+82.11	15.210	+.754	+.847	+.812
5	+306.50	+84.18	14.812	+.012	1.726	+.021
6	+162.84	+131.35	14.304	+.052	+.663	+.089
7	+673.08	+141.12	15.007	+.008	2.424	+.170
8	+710.96	+143.19	14.669	+.005	1.040	+.006
9	+758.48	+157.67	15.487	+.033	+.855	+.034
10	+896.80	+165.75	14.161	+.123	1.604	+.169
11	+233.45	+171.17	15.083	+.004	1.622	+.022
12	+337.90	+175.49	14.721	+.004	+.825	+.004
13	+495.81	+240.50	15.377	+.004	1.775	+.005
14	+68.88	+262.74	14.327	+.006	1.252	+.122
15	+859.22	+265.33	15.012	+.018	1.763	+.038
16	+993.53	+287.86	12.976	+.141	+.570	+.183
17	+438.93	+347.57	14.583	+.009	1.920	+.012
18	+458.27	+376.30	14.927	+.020	2.521	+.027
19	+87.02	+389.13	15.258	+.003	1.636	+.006
20	+8.71	+392.02	14.662	+.014	1.025	+.059
21	+142.12	+475.97	15.040	+.011	1.298	+.012
22	+188.37	+495.74	15.258	+.003	1.738	+.004
23	+262.50	+496.64	15.157	+.002	2.136	+.006
24	+41.62	+503.42	15.179	+.009	2.352	+.139
25	+14.47	+505.39	13.951	+.020	1.454	+.031
26	+858.68	+513.70	14.122	+.016	+.761	+.026
27	+233.41	+525.56	13.100	+.242	+.702	+.270
28	+284.82	+535.76	14.907	+.003	1.081	+.004
29	+298.46	+537.39	15.251	+.002	1.922	+.004
30	+128.84	+549.20	15.344	+.005	3.053	+.045
31	+903.81	+555.08	13.766	+.012	+.721	+.025
32	+362.93	+568.77	15.240	+.004	2.371	+.007
33	+749.61	+573.84	15.260	+.003	1.767	+.004
34	+521.90	+577.62	15.178	+.002	1.651	+.005
35	+432.14	+591.29	15.268	+.003	1.875	+.006
36	+626.51	+599.64	14.269	+.006	1.464	+.007
37	+502.37	+674.08	14.723	+.007	+.756	+.008
38	+247.69	+682.91	14.315	+.004	1.436	+.007
39	+127.93	+725.87	14.305	+.043	1.835	+.043
40	+856.68	+765.14	13.923	+.032	1.414	+.096
41	+868.43	+770.36	15.268	+.033	+.937	+.042
42	+665.69	+771.00	15.472	+.002	1.839	+.004
43	+795.66	+806.34	14.318	+.144	1.173	+.153
44	+520.07	+840.33	15.217	+.008	3.743	+.010
45	+395.07	+853.09	15.227	+.002	1.790	+.004
46	+61.91	+860.06	15.400	+.123	1.586	+.146
47	+696.63	+900.22	14.787	+.020	+.828	+.027
48	+894.31	+914.68	15.253	+.030	1.667	+.038
49	+920.96	+929.42	15.131	+.103	1.908	+.105
50	+276.19	+934.31	15.443	+.068	2.159	+.068
51	+730.08	+936.81	14.447	+.112	1.346	+.115
52	+261.07	+988.45	14.619	+.016	1.255	+.068
53	+558.02	1011.03	15.287	+.206	2.710	+.217

Obviously, there is a zero-point difference both in V and I. While the details of the calibration of OBB are not assessable for us, we want to cite evidence that our zero-points are not erroneous. We observed 47 Tuc in the same night and applied the same calibration as for NGC 6528. The CMD for 47 Tuc matched the Hesser et al. (1987) data excellently. The difference both in the HB brightnesses and in the RGB colours at the HB level is of the order of only 0.01 mag. Notice also that the gain in limiting magnitude with the long exposures on NGC 6528 is not so dramatic. It is the strong crowding around NGC 6528 which determines photometric errors and limiting magnitudes. Furthermore, a tendency for a non-linearity might be seen in the growth of the zero-point differences with decreasing brightness. We suspect that this may be related to the non-linearity of the RCA chips used by OBB, which were unkown at the time of observations (Abbott & Sinclaire 1993) (however, the referee expressed doubts that a non-linearity may result in such a large difference).

Comparison with the photographic data of van den Bergh & Younger (1979) is done for the V magnitudes. The deviations become larger at the limit of the photographic data ($\sim$ 17 mag), indicating a strong non-linearity in the photographic calibrations. The statistical results are given in Table 5. The referee pointed out that the cross-check present values-OBB-van den Bergh is not consistent, since OBB give −0.1 mag as the difference OBB-van den Berg. We are unable to resolve that inconsistency.

3. The colour-magnitude diagram of NGC 6528

3.1. General remarks, structural parameters, field population

Figure 2 shows a CMD of all 24999 stars that were identified independently on at least 4 frames. The $V-I$ scale is so compressed by the occurence of very red stars that features like the horizontal branch are not easily recognizable. It is clear, however, that the dominant population is not the cluster but the field population of the Galactic bulge. To maintain good legibility by avoiding an inconvenient compression of the $V-I$ scale, Fig. 5 plots only stars bluer than $V-I = 3.0$. No selection with respect to photometric errors was done to maintain completeness. The full list of stars (Table 6) is published in electronic form at CDS.

This CMD shows why the investigation of this cluster is so difficult. Practically all interesting structures in the CMD of NGC 6528 are contaminated by the field population. While the horizontal branch (HB) can be distinguished, the exact shape of the red giant branch (RGB) cannot be clearly identified. OBB found strong differential reddening in the area of NGC 6528 which further broadens the RGB and other features of the CMD. Also a "tilted" HB is recognisable, although less striking than in

Table 4. Statistical results of the difference ΔV and $\Delta V - I$ in the sense present minus Ortolani et al. (1992). V and $V - I$ are from the present photometry. The number of stars, N, used for the computation of the mean and standard deviations (σ) are also given. A few points discrepant by more than 3σ have been excluded

V	ΔV		$\Delta(V-I)$		$V-I$	$\Delta(V-I)$	
(mag)	Mean $\pm$ σ	N	Mean $\pm$ σ	N	(mag)	Mean $\pm$ σ	N
$14.0 - 16.0$	0.17 ± 0.01	35	0.01 ± 0.01	33	$0.5 - 1.2$	-0.02 ± 0.01	58
$16.0 - 16.5$	0.14 ± 0.01	56	-0.01 ± 0.01	55	$1.2 - 1.4$	0.01 ± 0.02	169
$16.5 - 17.0$	0.12 ± 0.01	68	-0.02 ± 0.01	71	$1.4 - 1.6$	0.09 ± 0.01	283
$17.0 - 17.5$	0.12 ± 0.01	172	-0.01 ± 0.01	186	$1.6 - 1.8$	0.04 ± 0.01	407
$17.5 - 18.0$	0.12 ± 0.01	108	0.01 ± 0.01	118	$1.8 - 2.0$	0.03 ± 0.01	224
$18.0 - 18.5$	0.14 ± 0.01	123	0.02 ± 0.01	126	$2.0 - 2.5$	0.01 ± 0.01	77
$18.5 - 19.0$	0.15 ± 0.01	124	0.05 ± 0.01	131	$2.5 - 6.0$	0.04 ± 0.03	30
$19.0 - 19.5$	0.18 ± 0.01	150	0.09 ± 0.01	157			
$19.5 - 20.0$	0.23 ± 0.02	153	0.17 ± 0.03	159			
$20.0 - 20.5$	0.24 ± 0.02	138	0.17 ± 0.03	145			
$20.5 - 21.0$	0.27 ± 0.03	74	0.21 ± 0.05	73			

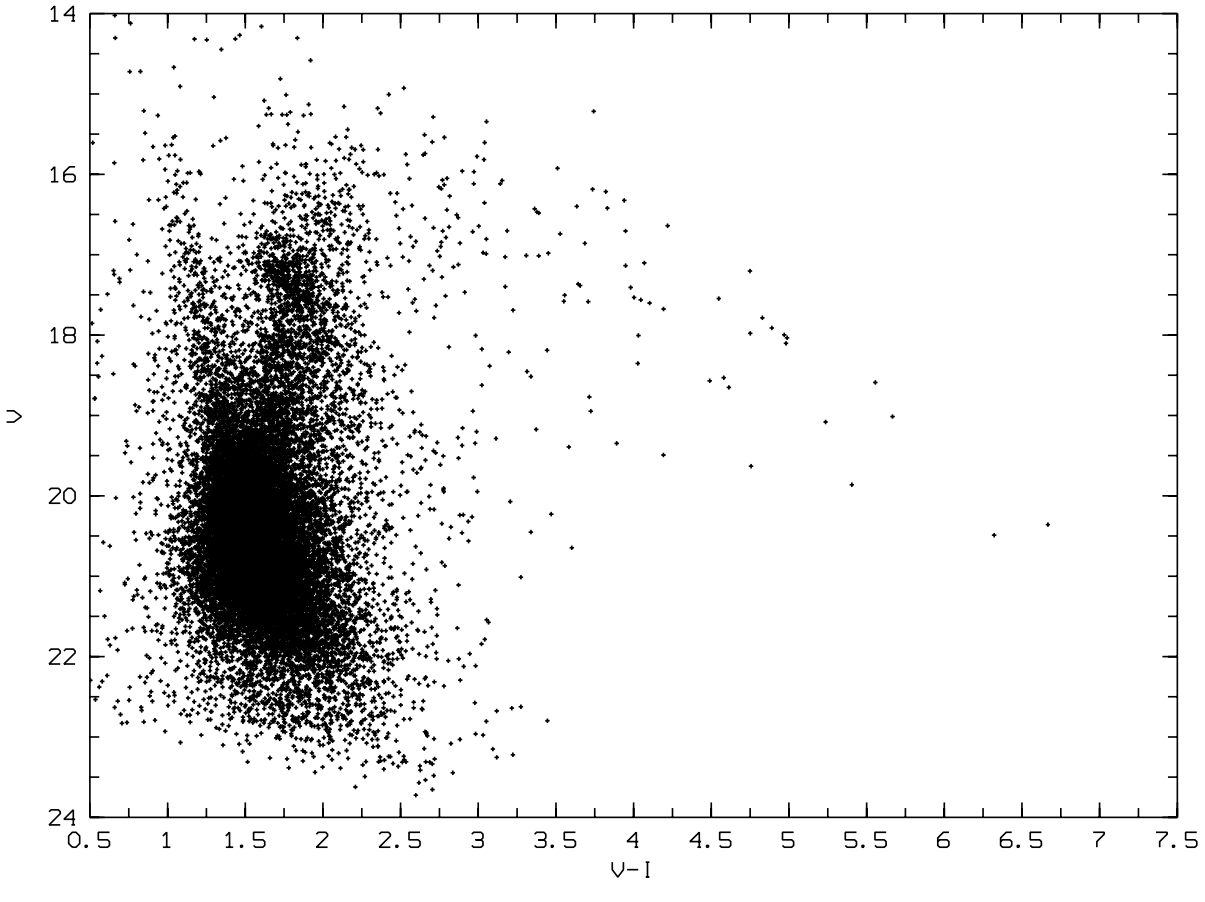

Fig. 2. The colour-magnitude diagram shows all 24999 stars, for which photometry could be obtained. The $V - I$ scale is strongly compressed by the occurence of very red stars, so that the CMD features of the cluster itself are hard to isolate. The cluster is embedded in a very rich population of field stars, which is the main obstacle for a proper derivation of cluster parameters. Triangles are those stars redder than $V - I = 3.0$, which are closer than $33.2''$ to the cluster center and accordingly have a high probability of being cluster members. They show that the cluster is situated in the foreground with respect to the red field star population

Table 5. Statistical results of the difference Δ in the sense present values minus van den Bergh & Younger (1979). The mean and standard deviations (σ) are based on N stars

V (mag)	ΔV Mean$\pm\sigma$	N
$15.0 - 16.0$	0.054 ± 0.044	16
$16.0 - 16.5$	0.071 ± 0.061	27
$16.5 - 17.0$	0.19 ± 0.18	20
$17.0 - 17.5$	0.49 ± 0.44	14

Table 6. This table is available at CDS. It contains 24999 stars with $x - y$-coordinates (the system of Fig. 3), V, $V - I$ and the respective errors, as well as the chi-values returned from DAOPHOT

other clusters like NGC 6553 (Subramaniam et al. 1997) or Terzan 5 (Grebel et al. 1995).
The turn-off region is reached in our photometry. It is at most 3.5 mag fainter than the HB, which is typical of old clusters (e.g., Buonanno et al. 1989), but it is completely hidden in the rich field. Here we skip any discussion of the TO location due to the superior data of HST (Ortolani et al. 1995).

The problem now consists of properly selecting stars with a high probability of being cluster members and statistically subtracting field stars in order to isolate the significant features of the CMD. A useful approach is to determine the radial distance beyond which the field population starts to dominate over the cluster population.

A King model reads (King 1962)

$$f(r) = K \cdot ((1 + (r/r_\mathrm{c})^2)^{-1/2} - (1 + (r_\mathrm{c}/r_\mathrm{t})^2)^{-1/2})^2$$

where K is the central stellar surface density (or surface brightness, respectively), r_c the core radius and r_t the tidal radius. Webbink (1985) quotes $r_\mathrm{c} = 0.27$ arcmin and $r_\mathrm{t} = 9.3$ arcmin, while Trager et al. (1993) give $r_\mathrm{c} = 0.08$ arcmin and $r_\mathrm{t} = 16.6$ arcmin. These differences illustrate the difficulties of deriving structural parameters for a cluster so strongly embedded in the field population. Our attempts to fit a King profile confirmed the degeneracy of the parameters. However, our area is quite limited so we cannot improve the parameter values.

We determined the radial profile of the surface density, selecting stars brighter than $V = 19$ mag, where we are complete except perhaps for the very center. We find for the central surface density 1300 ± 100 stars/square arcmin. The observed density profile together with two King models with the above parameters are given in Fig. 3. From this plot, the cluster and field densities are equal at a radius 1.1 arcmin. At 2.5 arcmin, the field density is already 8 times higher than the cluster density in case of the Trager et al. (1993) model.

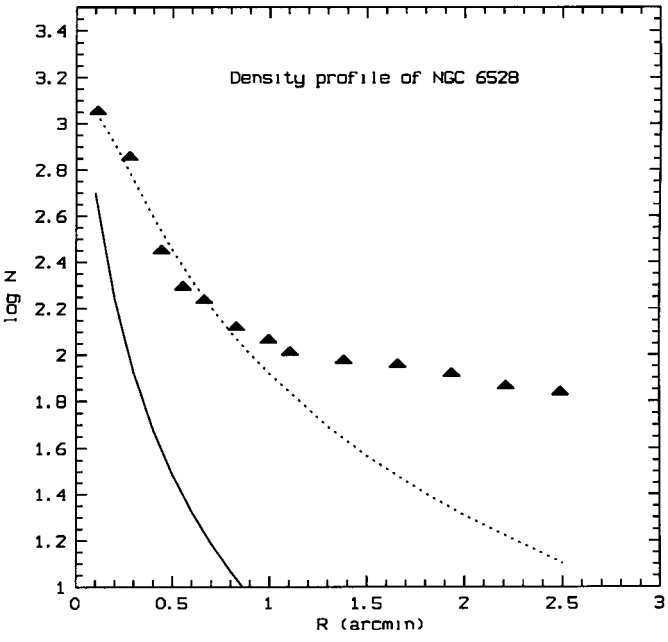

Fig. 3. This plot shows the observed stellar surface density (logarithm of stars brighter than $V = 19$ mag per square arcmin) as a function of radius (triangles). Also plotted are two King models with parameters quoted by Webbink (1985, solid line) and Trager et al. (1993, dotted line). At a radial distance of about 1.1 arcmin, the field population equals the cluster population. For constructing the field CMD, one should select stars with radial distances larger than 2.5 arcmin, where the cluster population is negligible

The CMD of the field population (Fig. 4) therefore consists of stars with radial distances larger than 2.5 arcmin.

3.2. The red giant branch (RGB) and the horizontal branch (HB)

The location of the RGB is the basis for estimation of the metallicity and reddening. In Fig. 5, it is difficult to locate the cluster RGB among the numerous field stars. We found that statistical field star subtraction in the region of the RGB does not give useful results due to small number statistics. Selection according to distance from the cluster worked much better.

We found that selecting the stars with distances less than 100 pix (0.553 arcmin) gave the best representation of the RGB. We are using this selection to define a fiducial for the RGB and the HB (both given in Fig. 6). Numerical values of the adopted fiducial are presented in Table 7.

It is interesting to note that the "tilt" of the HB recognizable in Fig. 5 vanishes in Fig. 6. Such tilts have been repeatedly reported for metal-rich clusters. Armandroff (1988) proposed differential reddening as the cause,

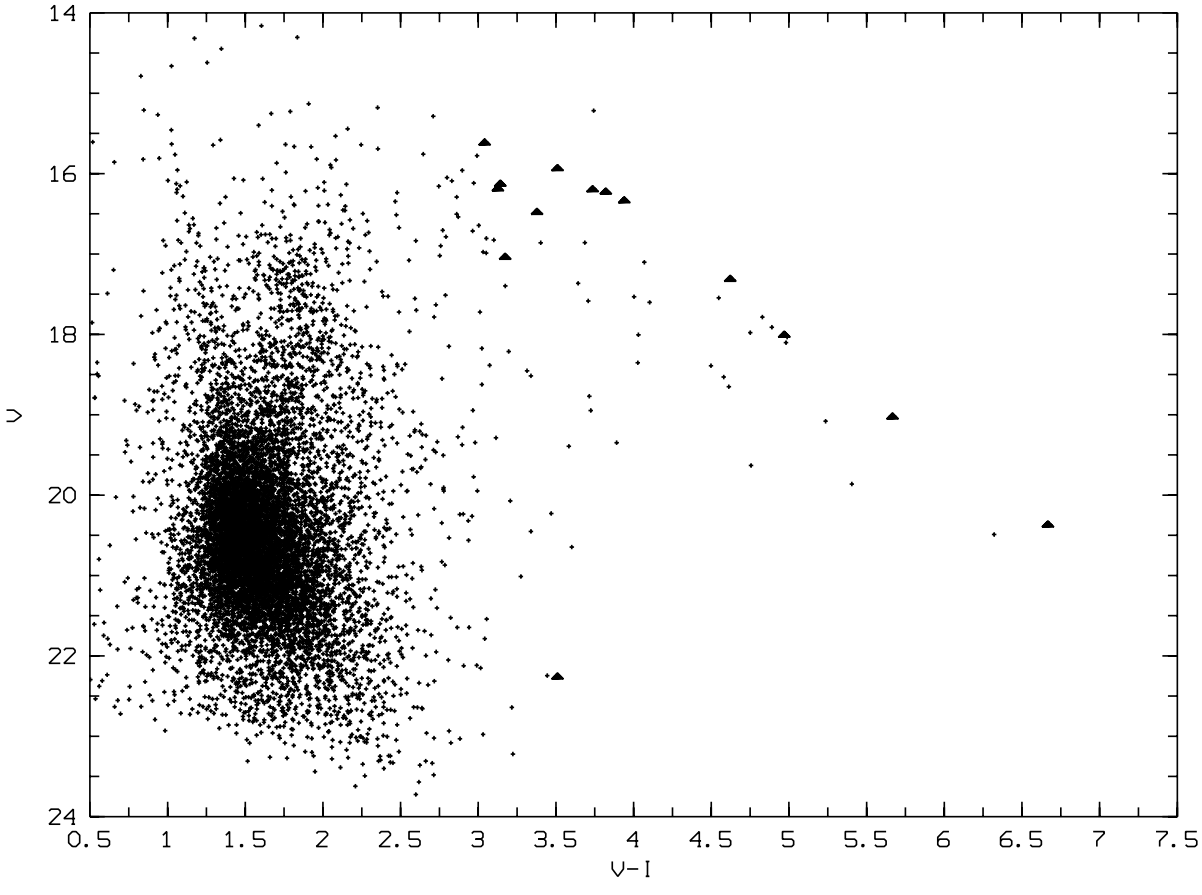

Fig. 4. The CMD of the field population around NGC 6528. We selected stars with radial distances larger than 2.5 arcmin to plot this diagram. Triangles are those stars redder than $V - I = 3.0$, which are closer than 33.2″ to the cluster center and accordingly have a high probability of being cluster members. One recognizes that the giant branch of NGC 6528 constitutes a brighter envelope to this star distribution and thus is located in the foreground

because the slope of the tilted feature resembles in the most striking cases the reddening vector. OBB already remarked that the HB gets more clumpy when HB stars near the cluster center are considered, which is confirmed by Fig. 5. This means that the tilt is mainly due to differential reddening in the field population.
On the other hand, NGC 6553 (Ortolani et al. 1991; Subramaniam et al. 1997) and Terzan 5 (Grebel et al. 1995) are examples, where the tilted HB branch is seemingly not induced by a smooth reddening gradient in the cluster field, but rather by extremely patchy reddening. This conjecture is strengthened by the fact that the "tilted" HB is more striking with increasing foreground reddening. However, a deeper discussion must include better data of highly reddened clusters.

3.3. The "curved giant branch"

Figure 2 shows many very red stars, the reddest ones have $V - I = 7$. They cannot be late M dwarfs since they are preferably found among the brighter stars, so they should be intrinsically bright. OBB interpret their occurence as a continuation of the RGB, caused by the high metallicity of the cluster and suggest that these stars are affected by strong blanketing.

The cluster membership of these stars is naturally of interest. If giants with such red $V - I$ colours occur in metal rich populations, we expect these stars to be present among to the Galactic bulge field stars as well. Indeed, the large majority of the stars redder than $V - I = 3.5$ does not show any concentration towards the cluster center and therefore likely belong to the bulge population.

However, a subsample have a high probability of being cluster members, since a selection according to radial distance (less than 60″ from the cluster center) is equivalent to the selection of the outer envelope of the distribution of the red stars (see Fig. 4). This implies that the cluster is not embedded in the field population, but is located in the foreground.

Garnavich et al. (1994) found a "curved giant branch" in the $V - I$, V-diagram of NGC 6791, a metal-rich old open cluster. Their calculations show that the decreasing V brightness can be understood simply as a consequence

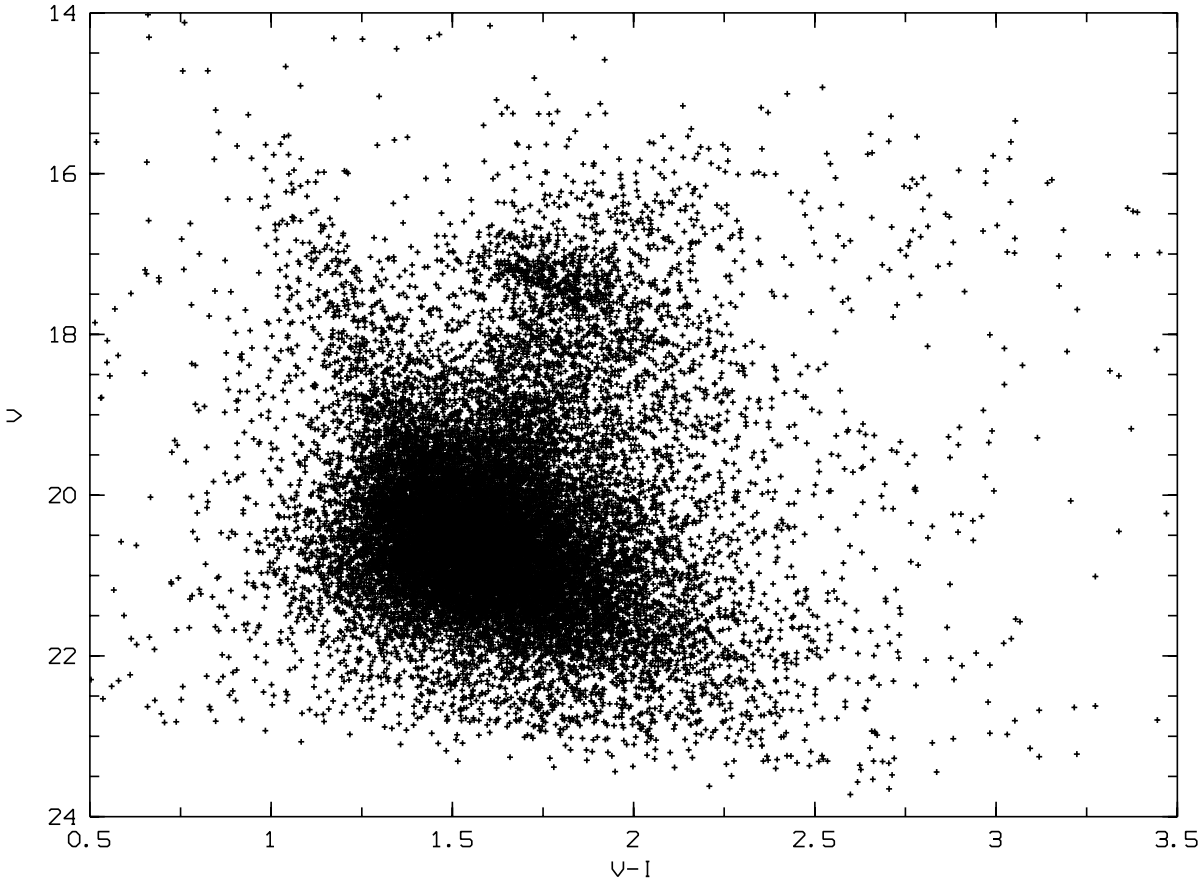

Fig. 5. This plot shows the CMD in $V, V-I$ of the NGC 6528 region containing only stars bluer than $V-I=3.5$. It is obvious that this diagram is overwhelmingly dominated by the population of the Galactic bulge. The HB of the cluster is discernible while the RGB cannot be clearly identified. The turn-off region is reached in our photometry but the turn-off itself is completely hidden in the field population

of a rapidly increasing bolometric correction. Quantitative theoretical statements concerning colours are difficult to make, since no detailed atmospheric models exist for very cool giants (c.f. Gustafsson & Jørgensen 1994), but models for cool dwarf stars show that already in the black or grey body approximation the stellar continuum at or below temperatures of 3000 K easily produces colours as red as $V-I \simeq 5$.

In Fig. 7 a theoretical isochrone from Bertelli et al. (1994) is overplotted. The isochrone has $Z=0.02$ and an age of 13.2 Gyr. The solid line is the RGB while the filled circles trace the AGB. It turns out that, if the reddest stars are indeed cluster members, the discrepancy between the theoretical isochrone and the actually observed locus starts at $V-I \simeq 4$. The evolutionary status of the red stars is not clear, but one may suspect in analogy to the theoretical isochrones that they are on the AGB rather than on the RGB.

To assess at least roughly their effect on integrated colours, we first calculate an integral $V-I$ colour of all stars in Fig. 2 and get 1.82 mag, while omitting the stars with $V-I > 3.5$ (as in Fig. 5) results in an integrated colour of 1.70 mag. This effect is plausibly even stronger in the infrared. So this red extension of the AGB/RGB stars must be taken into account, when modelling spectra of elliptical galaxies. See the contributions by Bruzual (1996), Worthey (1996), Chiosi (1996) for a deeper discussion of related problems.

3.4. The main sequence turn-off of NGC 6528

The question for the age of NGC 6528 is of high importance for the metal-rich bulge population of which NGC 6528 is a representative. Is NGC 6528 placed among those few globular clusters that are younger than the bulk of clusters, like Pal 12 (Gratton & Ortolani 1988) or Ruprecht 106 (Buonanno et al. 1990)? That "disk" clusters may be younger than halo clusters has been suggested for instance by Richtler et al. (1992) and Hatzidimitriou (1991). Ortolani et al. (1991) cited NGC 6553 as possibly younger. However, Richtler et al. (1994) showed that three other clusters, which had been classified as disk clusters (but in fact have properties more consistent with halo

clusters), could not be distinguished in age from the bulk of globular clusters.

After the first version of this paper had been submitted, Ortolani et al. (1996) published a CMD of NGC 6528, based on HST-data (WFPC2). Although the present data are the deepest so far obtained from the ground for NGC 6528, they are definitely less reliable concerning the turn-off location due to the strong crowding at the relevant magnitude level. Therefore we renounce a deeper discussion and simply refer to Ortolani et al. who found that NGC 6528 is indistinguishable in age from the metal-poorer clusters in the galactic halo.

Table 7. Our fiducial for the RGB of NGC 6528 derived by radius selection

$V-I$	V
2.909	15.489
2.645	15.672
2.309	16.120
2.151	16.486
2.003	16.818
1.887	17.317
1.835	17.616
1.787	17.998
1.719	18.663
1.640	19.410
1.645	19.826
1.592	20.125
1.661	17.217
1.698	17.217
1.719	17.217
1.740	17.217
1.761	17.217
1.745	17.234
1.724	17.234
1.703	17.234
1.692	17.234

3.5. Reddening & Metallicity

Sarajedini (1994) devised a simple method to derive metallicity and reddening simultaneously from a V, $V-I$ diagram by using two metallicity indicators, $\Delta V_{1.2}$, the magnitude difference between HB and RGB at the unreddened $V-I$ colour 1.2, and $(V-I)_{0,\mathrm{g}}$, the (unreddened) $V-I$ colour of the RGB at the HB magnitude level. These metallicity indicators depend in different ways on the reddening. Thus we can regard reddening and metallicity to be determined, if both indicators give the same metallicity for the same reddening. However, a direct application is not possible since in Sarajedini's calibration, 47 Tuc appears with -0.7 dex as the most metal-rich cluster, whereas one wants to have a calibration extended to at least solar metallicity.

At present this is practically impossible to do in a purely empirical way. There are simply no V, $V-I$ CMDs for clusters suitable for inclusion in the metal-rich domain as a supplement to Sarajedini's calibration. But there are also only a few theoretical isochrones available for clusters this metal-rich. The only published $V-I$ isochrones for old and metal-rich clusters that we are aware of are those of Tripicco et al. (1995) and from Bertelli et al. (1994). Our approach is therefore to use these isochrones like empirically determined CMD loci and supplement the calibration set of Sarajenini.

3.5.1. The isochrones of Tripicco et al. (1995)

The 12 Gyr, solar metallicity isochrone of Tripicco et al. (1995) agrees very well with a linear extrapolation of Sarajedini's relations and its inclusion has only a little effect on the coefficients. For this isochrone, $(V-I)_{0,\mathrm{g}} = 1.10$ and $\Delta V_{1.2} = 0.45$. Measuring these indicators, we adopted for the brightness of the HB $M_V = 1.05$ mag, as indicated by the red part of the theoretical HB of Tripicco et al. (1995). A linear regression then leads to

$$[M/H] = (10.30 \pm 0.47) \cdot (V-I)_{0,\mathrm{g}} - (11.23 \pm 0.07)$$

and

$$[M/H] = (-1.06 \pm 0.05) \cdot \Delta V_{1.2} + (0.5 \pm 0.10).$$

These relations can now be used individually to plot reddening against metallicity, using the proper values for NGC 6528, for which we adopted $V - I_{\mathrm{g}} = 1.9$ and the numbers given in Table 8. These two lines then intersect at a certain pair of values that we regard to be the cluster reddening and metallicity. It is apparent that the main uncertainty is introduced by $V - I_{0,\mathrm{g}}$, which loses sensitivity in the metal-rich domain. We conclude from this method that the reddening of NGC 6528 is $E(V-I) = 0.8$ and a metallicity of $+0.1$ dex.

Table 8. This table gives the magnitude difference between the corresponding points on the RGB and the HB for different $V-I$ colours. Note that $V-I = 1.2 + E(V-I)$, so the table gives $\Delta V_{1.2}$ for different values of the reddening

$V-I$	ΔV
2.62	0.06
2.72	0.39
2.80	0.64
2.95	1.00
1.16	1.16

3.5.2. The Bertelli et al. (1994) isochrones

If Sarajedini's relation is supplemented with the aid of the Bertelli et al. (1994) isochrones, the linearity is lost

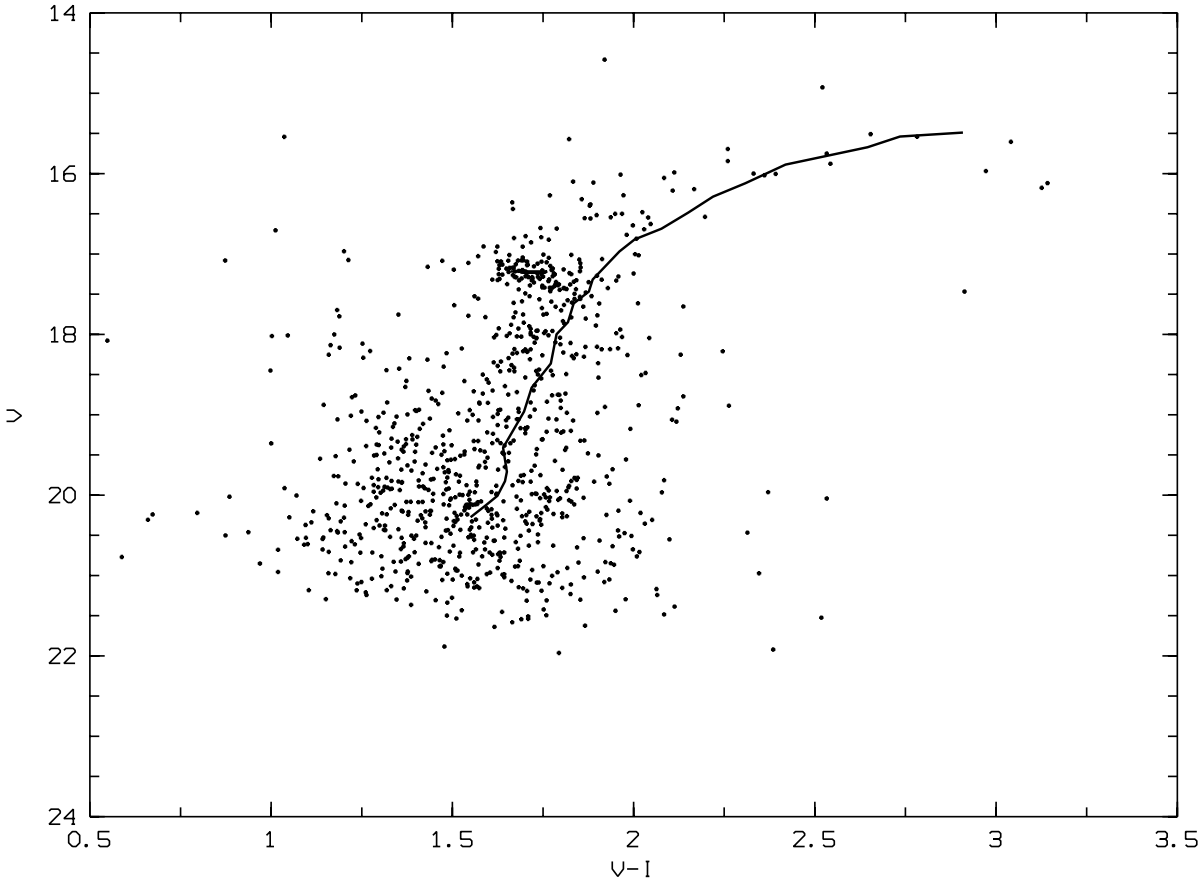

Fig. 6. CMD resulting from a selection with of stars closer than 33.2″ to the cluster center. This selection was used to define a fiducial for the RGB and the HB, which is overplotted (filled circles). It can be seen that the apparent "tilt" of the HB, which may be present in Fig. 2 vanishes if the stars on the HB have a high probability of being cluster members

and a significant curvature is introduced. We chose the [13.2 Gy, $Z = 0.02$] isochrone for extrapolating to solar metallicity.

For this isochrone, $(V-I)_{0,\mathrm{g}} = 1.3$ and $\Delta V_{1.2} = -0.75$. Including this point in Sarajedini's relation, leads to

$$[M/H] = (10.30 \pm 0.47) \cdot (V-I)_{0,\mathrm{g}} - (11.23 \pm 0.07)$$

and

$$[M/H] = (-1.06 \pm 0.05) \cdot \Delta V_{1.2} + (0.5 \pm 0.10).$$

Applying the above relations, our result for reddening and metallicity is $E(V-I) = 0.6$ and $[M/H] = -0.4$ dex. The uncertainty expressed by this difference can presently not be avoided.

3.6. Distance

Calculating the distance based on HB brightness, we have to adopt a relation between brightness and metallicity for HB stars (basically for RR Lyrae stars). A recent compilation of related work has been given by Chaboyer et al. (1996). Their preferred relation is

$$M_V = 0.2 * [\mathrm{Fe/H}] + 0.98.$$

To span a representative range of values occurring in the literature, we also adopted the relation favoured by Nemec et al. (1994):

$$M_V = 0.32 * [\mathrm{Fe/H}] + 1.19.$$

Moreover, the absorption depends on the colour of the star considered. Assuming $A_V = 3.4 \cdot E(B-V)$ (Grebel & Roberts 1995) as the appropriate relation for our value of $(B-V)_{0,\mathrm{g}}$, and $E(V-I) = 1.31 \cdot E(B-V)$, we get the values for M_V(HB), absorption, distance modulus and corresponding distance listed in Table 10. This table shows the full dilemma of distance determination of reddened globular clusters. We note that the ration $A_V/E(B-V)$ might also be discussed. In case of NGC 6528, a change of 0.3 would cause a shift of 0.25 mag in the distance modulus. Formally, there is no hard reason to consider any of these values as being more reliable than the others. However, since the structure of the CMD sets the cluster in the foreground, the high values are not probable. The recent investigation by Fusi Pecci et al. (1996) of M 31 globular clusters argues in favour of the Chaboyer et al. relation, so the distance value of 6.6 kpc might be preferred. One

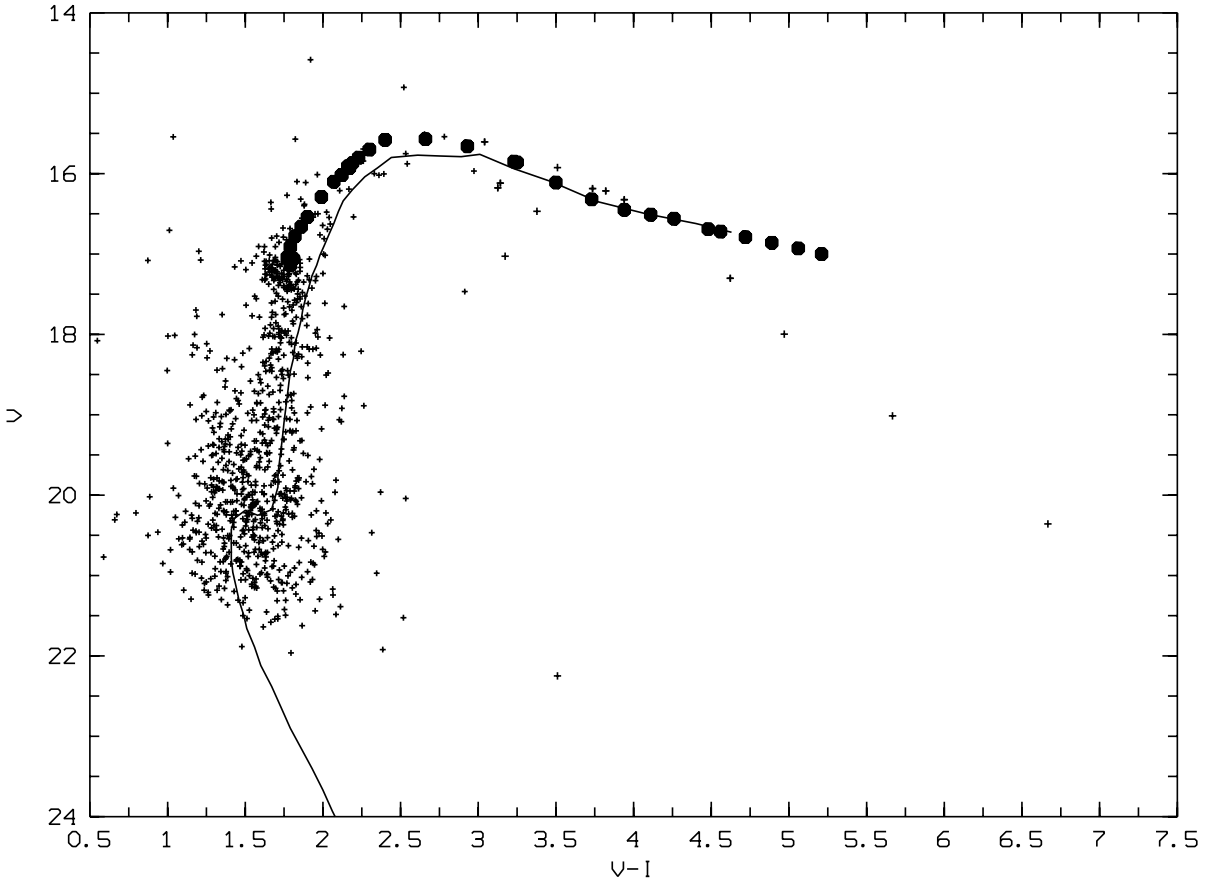

Fig. 7. This plot shows the full colour range of stars with the selection of being closer than 33.2″ to the cluster center. Overplotted is a theoretical isochrone from Bertelli et al. (1994) with an age of 13.2 Gy and solar metallicity, including the Red Giant Branch (RGB, solid line) and the Asymptotic Giant Branch (AGB, filled circles). While the isochrone traces the RGB and the AGB well to $V - I \simeq 4$, they deviate at redder colours and also do not cover the full extension of the CMD. Whether the reddest stars are RGB or AGB stars, is unclear

Table 9. Measured parameters for NGC 6528 using an extrapolation of Sarajedini's (1994) calibration with isochrones of Bertelli et al. (1994) (B) and Tripicco et al. (1995) (T)

m_V(HB)	$V - I_g$	$E(V-I)$(T)	$[M/H]$ (T)	$E(V-I)$(B)	$[M/H]$ (B)
17.21 ± 0.05	1.9 ± 0.05	0.8	+0.1 dex	0.6	−0.4 dex

notes that the external error is much more dependent on the uncertain metallicity, absorption and HB brightness than on the photometric errors.

4. Discussion and conclusions

It is clear that NGC 6528 belongs to the most metal-rich globular clusters in the Milky Way.

Minniti (1995) compiled evidence that the metal-rich clusters termed "disk clusters" by Zinn (1985) do belong to the Milky Way bulge rather than to the thick disk. While there may be still halo clusters among this sample, for instance NGC 6624, 6637 and 6496 (Richtler et al. 1994), NGC 6528 possesses all properties consistent with an origin in the Galactic bulge, as was already pointed out by OBB and by Ortolani et al. (1995), including its old age.

NGC 6528 possesses a further property that makes an origin as an object with disk properties very unlikey, namely its radial velocity. Zinn & West (1984) quote a value of +160 km/s, the value of Armandroff & Zinn (1988) is even higher (+180 km/s). Given the fact that the cluster is almost projected onto the Galactic center, a circular orbit can be excluded, since this would imply a an almost vanishing radial component. The circular velocity assuming at the cluster's galactocentric distance is about 200 km/s and thus still the cluster must have an

Table 10. Adopted and derived parameters for NGC 6528 using different relations (see text) between HB brightness and metallicity. It is indicated whether the Chaboyer et al. (1996) (C) or the Nemec et al. (1994) (N) relation is used. It becomes clear that the external distance uncertainty is completely dominated by these relations and the uncertain absorption. For the calculation of the galactocentric distance, we assumed 8 kpc as the distance from the sun to the Galactic Center

$E(V-I)$	[Fe/H]	M_V(HB)	A_V	$m-M$	D[kpc]	z[kpc]	$D_{\rm GC}$
0.8	+0.1	1.22 (N)	2.08	13.91	6.0	0.4	2.0
0.8	+0.1	1.02 (C)	2.08	14.11	6.6	0.5	1.5
0.6	−0.4	1.06 (N)	1.55	14.60	8.3	0.6	0.7
0.6	−0.4	0.90 (C)	1.55	14.76	8.9	0.7	1.1

appreciable radial component towards us. A distance of 7.5 kpc, as given by OBB, means a galactocentric distance of only 0.7 kpc and one could reasonably assume that the cluster then would be close to its perigalacticon. However, this distance does not fit to our finding that the cluster is located in the foreground with respect to the red field stars. Moreover, an orbit with low excentricity so close to the center would probably not allow the cluster to survive dynamically for more than 10 Gyr.

That leads to the conclusion that the cluster orbit must be highly excentric, a further reason against an origin in the disk. On the other hand, its high metallicity is an argument for a birth place not too far away from the Galactic center, i.e. in the bulge. One is tempted to speculate that the conditions at birth which put this cluster with a large initial velocity into an eccentric orbit, may best be realised in a chaotic environment with gaseous subunits of the central protogalaxy strongly interacting. This would fit to the meanwhile numerous observations that globular clusters are formed in dynamically hot environments, such as galaxy interactions.

Note added in proof: Meanwhile, the Hipparcos data have been used to recalibrate the relation between metallicity and HB-brightness of globular clusters. The presently available results from different workers differ by about 0.2 mag, thus a final answer is still pending (e.g. Gratton, et al., 1997, ApJ (in press); Pont, et al., 1997, A&A (in press)).

Acknowledgements. T.R. wants to thank the Humboldt Foundation for generous support and the Indian Institute of Astrophysics for hospitality and financial support. EKG acknowledges support by a fellowship of the DFG Graduiertenkolleg "Magellanic Clouds" and by the German Space Agency (DARA) (grant 05 OR 9103 0). Furthermore, we thank S. Ortolani for mailing his photometric data. This research has made use of the Simbad database, operated at CDS, Strasbourg, France.

References

Abbott T.M.C., Sinclaire P., 1993, The Messenger 73, 17
Armandroff T.E., 1988, AJ 96, 588
Armandroff T.E., 1993, in "The Globular cluster - Galaxy Connection", A.S.P. Conf. Ser. 48, Smith G.H. and Brodie J.P. (eds.). BookCrafters, Inc., San Francisco
Armandroff T.E., Zinn R., 1988, AJ 96, 92
Bergbusch P.A., VandenBerg D.A., 1992, ApJS 81, 163
Bertelli G., Bressan A., Chiosi C., Fagotto F., Nasi E., 1994, A&AS 106, 275
Buonanno R., Corsi C.E., Fusi Pecci F., 1989, A&A 216, 80
Bruzual G, 1995, in "New Light on Galaxy Evolution", IAU Symp. 171, Bender. R. and Davies R.L., (eds.). Kluwer Academic Publishers, Dordrecht, p. 61
Buonanno R., Buscema G., Fusi Pecci F., Richer H.B., Burkert A., Smith G., 1997, ApJ 474, L15
Chaboyer B., Demarque P., Sarajedini A., 1996, ApJ 459, 558
Chiosi C., 1995, in "New Light on Galaxy Evolution", IAU Symp. 171, Bender R. and. Davies R.L. (eds.). Kluwer Academic Publishers, Dordrecht, p. 75
Da Costa G.S., Armandroff T.E., 1990, AJ 100, 162
Fahlman G.G., 1990, AJ 100, 1811
Francois P., 1991, A&A 247, 56
Fusi Pecci F., Buonanno R., Cacciari C., et al., 1996, AJ 112, 1461
Fullton L.K., Carney B.W., Olszewski E.W., et al., 1995, AJ 110, 652
Garnavich P.M., VandenBerg D.A., Zurek D.R., Hesser J.E., 1994, AJ 107, 1097
Gratton R., Ortolani S., 1988, A&A 73, 137
Grebel E.K., Roberts W.J., van de Rydt F., 1994, in CTIO/ESO Workshop "The Local Group. Comparative and Global Properties", ESO Conference & Workshop Proceedings # 51, Layden A., Smith R.C. & Storm J., (eds.). La Serena, p. 148
Grebel E.K., Roberts W.J., 1995, A&AS 109, 293
Grebel E.K., Brandner W., Richtler T., Subramaniam A., Sagar R., 1995, BAAS 27, 1404
Gustafsson B., Jørgensen U.G., 1994, A&AR 6, 19
Hatzidimitriou D., 1991, MNRAS 251, 545
Hesser J., Harris W.E., VandenBerg D.A., et al., 1987, PASP 99, 739
King I.R., 1962, AJ 67, 471
Landolt A., 1992, AJ 104, 340
Minniti D., 1995, AJ 109, 1663
Nemec J.M., Nemec A.F.L., Lutz T.E., 1994, AJ 108, 222
Ortolani S., Barbuy B., Bica E., 1991, A&A 249, 310
Ortolani S., Bica E., Barbuy B., 1992, A&AS 92, 441 (OBB)

Richtler T., Grebel E.K., Seggewiss W., 1992, in "Stellar Populations of Galaxies", IAU Symp. 149, Barbuy B. & Renzini A. (eds.). Kluwer, Dordrecht, p. 477
Richtler T., Grebel E.K., Seggewiss W., 1994, A&A 290, 412
Sarajedini A., 1994, AJ 107, 618
Stetson P.B., 1990 (private communication)
Stetson P.B., 1992, DAOPHOT II Manual
Subramaniam A., Sagar R., Richtler T., Grebel E.K., 1997 (NGC 6553) (in preparation)
Trager S.C., Djorgovski S., King I.R., 1993, in "Structure and Dynamics of Globular Clusters", A.S.P. Conf. Ser. 50, Djorgovski S.G. and Meylan G. (eds). BookCrafters, Inc., San Francisco, p. 347
Tripicco M., Bell R.A., Dorman B., Hufnagel B., 1995, AJ 109, 1697 (TBDH)
van den Bergh S., Younger F., 1979, AJ 84, 1305
Webbink R.F., 1985, in "Dynamics of Star Clusters", IAU Symp. 113, Goodman J. (ed.). Reidel, Dordrecht, p. 541
Worthey G., 1995, in "New Light on Galaxy Evolution", IAU Symp. 171, Bender R. and Davies R.L. (eds.). Kluwer Academic Publishers, Dordrecht, p. 71
Zinn R., 1985, ApJ 293, 424
Zinn R., West M., 1984, ApJS 55, 45